Marine Structures 23 (2010) 115–130

Contents lists available at ScienceDirect

Marine Structures

journal homepage: www.elsevier.com/locate/marstruc

Full-scale fatigue tests of ship structures to validate the S–N approaches for fatigue strength assessment

Wolfgang Fricke*, Hans Paetzold

Institute of Ship Structural Design and Analysis, Hamburg University of Technology (TUHH), Schwarzenbergstr. 95c, 21073 Hamburg, Germany

ARTICLE INFO

Article history:
Received 23 July 2009
Accepted 25 January 2010

Keywords:
Ship structure
Welded detail
FEM
Fatigue strength assessment
Structural hot-spot stress
Effective notch stress

ABSTRACT

Ships belong to those welded structures which are prone to fatigue due to high cyclic loads. Different approaches exist for the fatigue strength assessment which are varying between the industrial sectors. Therefore, deeper fatigue strength investigations were performed in Germany within an industry-wide joint research project aiming at the harmonization of the approaches. Regarding ship structures, two types were selected for full-scale tests. The first concerned web frame corners being typical for roll-on/roll-off ships (ro/ro) ships, from which three models were tested under constant amplitude loading. The second type was the intersection between longitudinals and transverse web frames, which recently showed fatigue failures in containerships. Five models were tested, three under constant and two under variable amplitude loading. All tests showed a relatively long crack propagation phase after first cracks had appeared, calling for a reasonable failure criterion. For the numerical analysis, the structural hot-spot stress as well as the effective notch stress approach have been applied. The latter allows the consideration of the weld shape which could partly explain differences in the observed and calculated failure behaviour. Another factor is the distribution of welding-induced residual stresses, which obviously affected the failure behaviour in the web frame corner as well. Insofar the investigations give a good insight into the strength behaviour of complex welded structures and into current problems and opportunities offered by numerical analyses.

* Corresponding author. Tel.: +49 40 42878 6089; fax: +49 40 42878 6090.
E-mail address: w.fricke@tu-harburg.de (W. Fricke).

0951-8339/$ – see front matter © 2010 Elsevier Ltd. All rights reserved.
doi:10.1016/j.marstruc.2010.01.004

1. Introduction

Fatigue has been an important design criteria in shipbuilding for a long time [1–3]. This concerns both the longitudinal members such as deck, bottom and side structures, for instance attachments at longitudinals, as well as transverse members such as the connections of deep web frames. Cyclic stresses are primarily induced by fluctuating wave pressure and ship motions.

The complexity of ship structures creates problems during the proof of sufficient fatigue strength. These lie on the one hand in the numerical analysis of stresses in accordance with the approach chosen for the assessment, which are in most cases the nominal and the structural hot-spot stress approaches [4]. As mainly shell models are used, the appropriate modelling of welded joints and the stress evaluation are not easy [5–8]. On the other hand, the assumption of load spectra contains large uncertainties with respect to the expected operation profile. In the new Common Structural Rules for tankers and bulk carriers, much effort is spent to consider different wave situations as well as loading conditions and hereby mean stresses [9].

Internationally, different views and solution strategies have been established to ensure a sufficient fatigue strength, which are reflected in varying rules and guidelines. This is similar also in other industrial sectors, so that a cluster project was initiated a few years ago under supervision of the German Welding Society (DVS), which was intended to validate, harmonize and probably improve the "Strength assessment concepts for cyclic loaded welded structures" on the basis of experimental investigations of full- and small-scale fatigue specimens. The partners included six research institutions, which investigated structural components from shipbuilding, automotive and railway engineering as well as mechanical engineering.

The different structures included different materials and welding processes. Shipbuilding is represented by relatively thick structures compared to the other industrial sectors. The full-scale models concerned web frame corners being typical for ro/ro ships and intersections between longitudinals and transverse webs in containerships, where fatigue failures have recently occurred [10]. Parallel to the full-scale tests, small-scale specimens were investigated, which represent the fatigue-critical detail. This should establish the link to the fatigue test results which are the basis of the well-known fatigue classes in the nominal stress approach [6,8,11].

Generally it was planned to apply all available techniques to characterize the test models as far as practicable in order to record most of the influence factors of fatigue. This includes the measurement of weld profiles and residual stresses.

In the following, the experimental and numerical investigations on the full-scale test models are described and conclusions drawn. Further details can be found in [12].

2. Investigation of the web frame corner

2.1. Test models

On the basis of current ro/ro ships, a corner connecting the web frames of the ship's side and deck was selected. The web frames are primary structural members in the transverse ship sections. They are mainly subjected to bending due to static and dynamic loads, e. g. during rolling.

The depth of the T-shaped web frames is 0.6 m and the flanges consist of flat bars 250×20 (continuous flange) and 200×20 (interrupted flange). The test model in Fig. 1 contains two web frame corners. A diagonally acting hydraulic cylinder (Fig. 2) creates a bending moment together with an axial and a shear force in both frames. The latter produce relatively small stresses so that the frame is mainly subjected to bending.

In total three models were built, two in the usual configuration, while the third contained additional diagonal stiffeners on the web in the intersection area which were connected with full-penetration welds at their ends. The material was higher-tensile steel S355. All models were fabricated in the usual way by placing at first the individual frames on the plates and afterwards connecting the 'block joint' (between the white and coloured parts in Fig. 1). Here, the 10 mm thick web was MAG-welded first, before the flange 200×20 was connected by full-penetration welding. This cruciform joint was expected to be the fatigue-critical point.

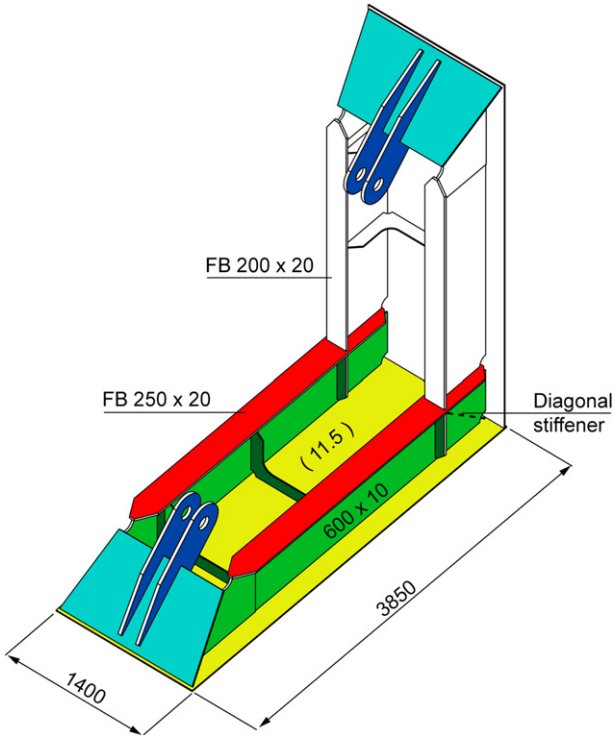

Fig. 1. Web frame corner investigated.

2.2. Fatigue tests

Preceding finite element analyses had shown that due to the cut-out for welding relatively large stresses occur at several weld toes. Apart from the two weld toes at the end of the flange 200×20, which are denoted HS1 and HS2 in Fig. 3 (HS means hot spot), the weld toes HS3 and HS4 are highly stressed at the ends of the cut-out for welding. Here, strain gauges were applied in order to evaluate the structural stress. The highest stress was found at HS2.

The fatigue tests were performed with constant amplitude loading and a load ratio of $R \approx 0$. The load range in the models was between $\Delta F = 230$ kN and 280 kN. The corresponding nominal stress in the flange varied from 81.9 N/mm^2 to 99.4 N/mm^2.

Surprisingly, the first crack was observed in all models not at HS2, but at HS3. However, it lasted very long until the crack penetrated through the flange thickness. Fig. 4 illustrates the development of the crack length measured on the inner surface of the flange. After penetrating the flange (at a crack length of approx. 50 mm), the crack propagation rate increased considerably.

During the tests, cracks were observed also at other hot-spots. In the first two models, the second crack appeared at HS4, where also one crack initiated from the non-welded root face. In the third model with the diagonal stiffener, the second crack appeared at HS2 and grew so quickly that it determined finally the failure of the model, characterized by a separation of more that half the flange area.

For a comparison of the endured load cycles with design S–N curves, a specific failure criterion needs to be defined, which is problematic in view of the long crack propagation phase. Frequently, the penetration of a wall thickness is chosen as failure because a leak is present and the crack propagation

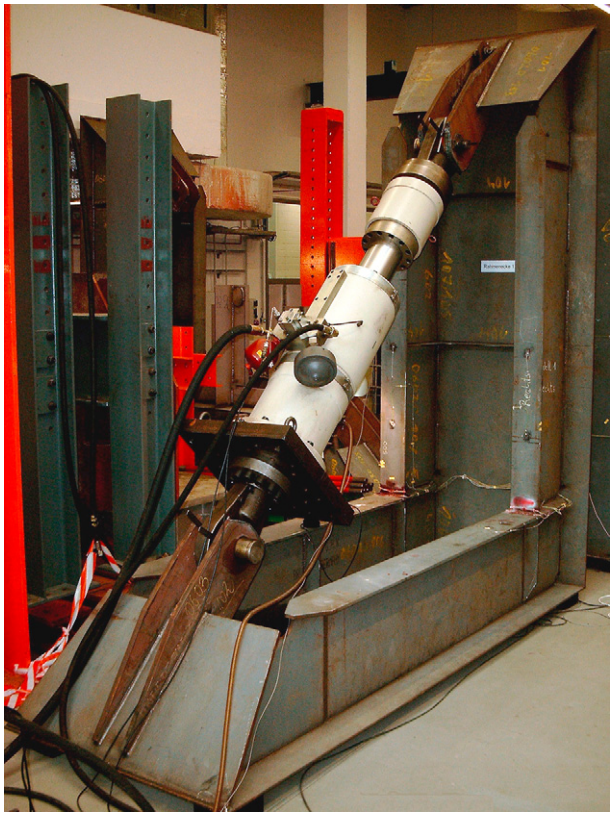

Fig. 2. Test set-up.

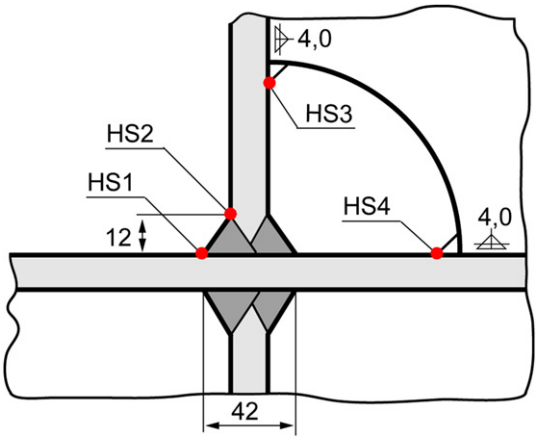

Fig. 3. Critical part of the web frame corner with hot-spots HS1–HS4.

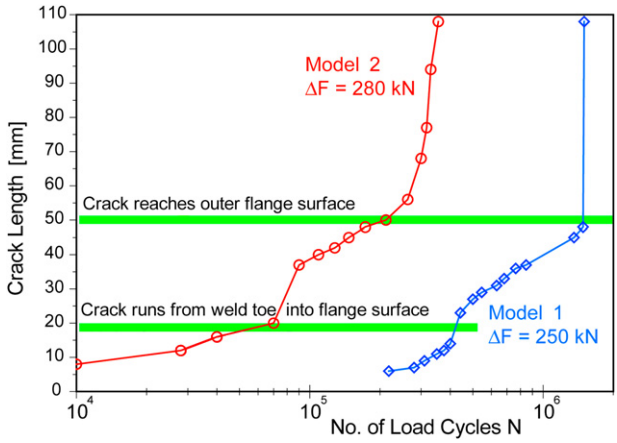

Fig. 4. Typical crack development at HS3.

rate is then considerably increasing. For practical reasons, a crack length corresponding to the plate thickness, i.e. 20 mm, is chosen, which is somewhat more conservative than the aforementioned criterion. The corresponding fatigue lives are summarized in Table 1.

2.3. Residual stress measurement

Originally it was planned to perform measurements with the X-ray technique on the surface of the flanges. As the fatigue tests showed the first cracks at the ends of the cut-out for welding, where measurements with the X-ray technique are not possible, also the destructive cut-out technique was chosen for the measurement. However, this required a separate model representing the critical area, see Fig. 5. The extension of the model was chosen such that similar residual stresses could be expected as in the large model. A corresponding weld sequence was chosen.

For the measurement, strain gauges were applied at the locations of interest and the strain was measured before and after arranging saw-cuts around them. In this way, the residual stresses were measured being released during the cutting process.

The results of both measurements in Fig. 6 show generally tensile residual stresses. The highest stresses were found close to HS3. These are obviously caused by the welding sequence and could explain the unexpected structural behaviour observed during the fatigue tests. However, also the cyclic loading should be considered as the yield stress is exceeded in the notch, relaxing the residual stresses.

2.4. Finite element analyses

Parallel to the experimental investigations, extensive finite element analyses were performed. On the one hand, a comparison with the measured nominal and structural strains was intended in order to validate the results. On the other hand, also the effective notch stresses should be determined in order to check their applicability to the fatigue assessment of web frame corners.

Table 1
Endured load cycles *N* in the web frame models when reaching a crack length of 20 mm.

Model	Δ*F* (kN)	*N* (left frame)	*N* (right frame)
1	250	400.000	420.000
2	280	80.000	70.000
3	230	370.000	200.000

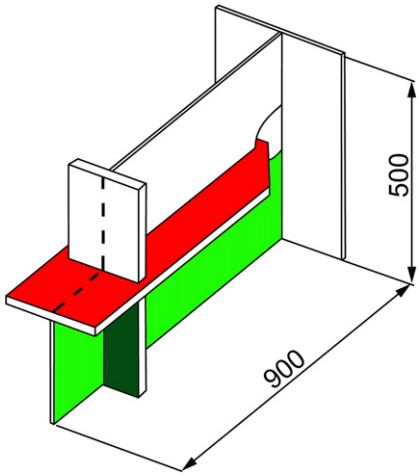

Fig. 5. Separate model for the residual stress measurement.

In order to compute the structural stresses, the overall model shown in Fig. 7 was established using solid elements with 20 nodes. The element sizes correspond to the recommendations in [4] for the stress extrapolation to the hot-spots. Two models were created:

- Model A with the nominal weld geometry, and
- Model B with the actual weld leg lengths.

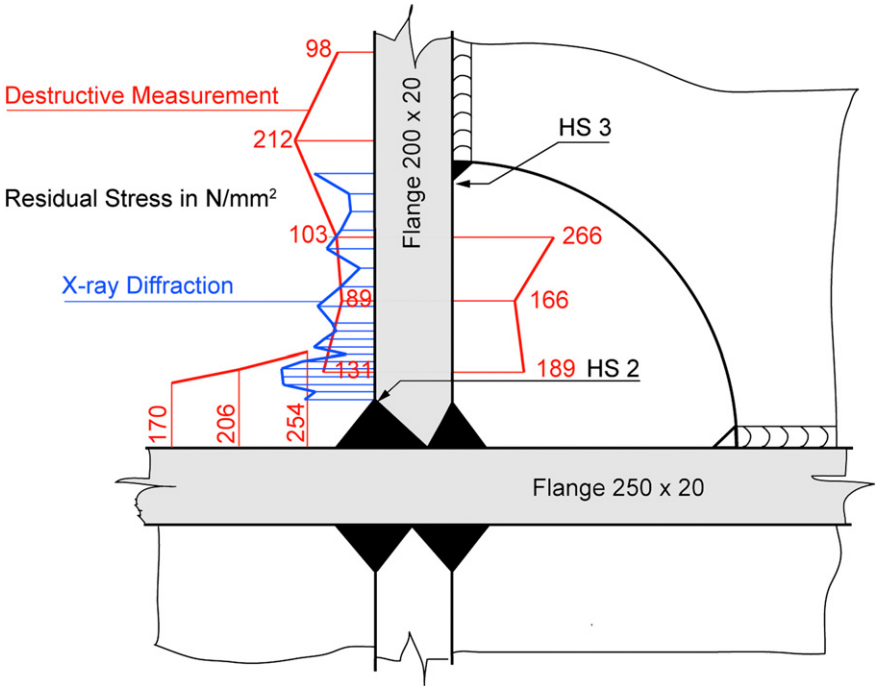

Fig. 6. Measured residual stresses.

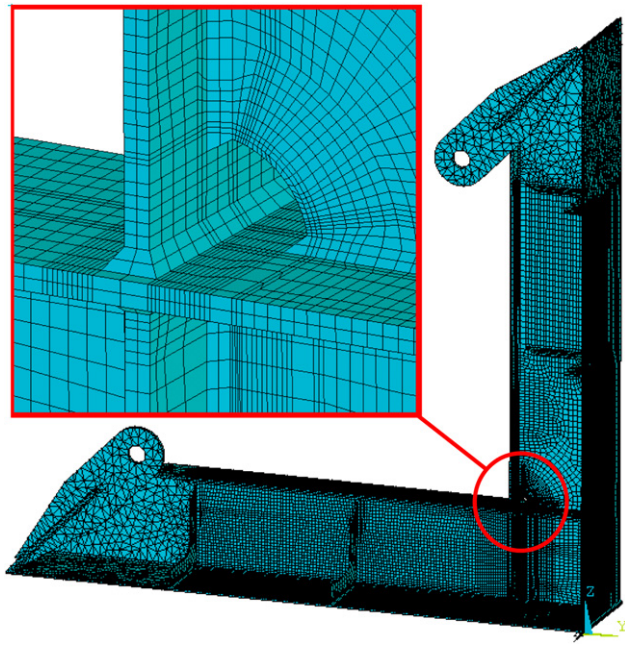

Fig. 7. Finite element model of the web frame corner for the structural stress analysis.

Fig. 8 illustrates the geometries together with a third model C which contains the actual weld toe radii for the notch stress calculation.

The structural hot-spot stress was determined at HS1 - HS4 by extrapolating the surface stresses at reference points located 0.4*t* and 1.0*t* away from the weld toe as recommended in [4] and [11].

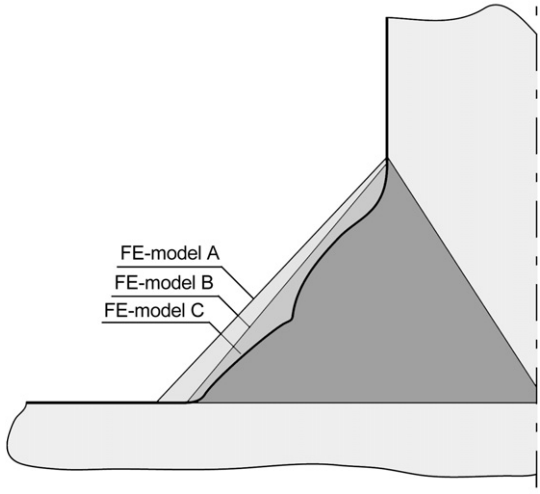

Fig. 8. Weld geometries investigated.

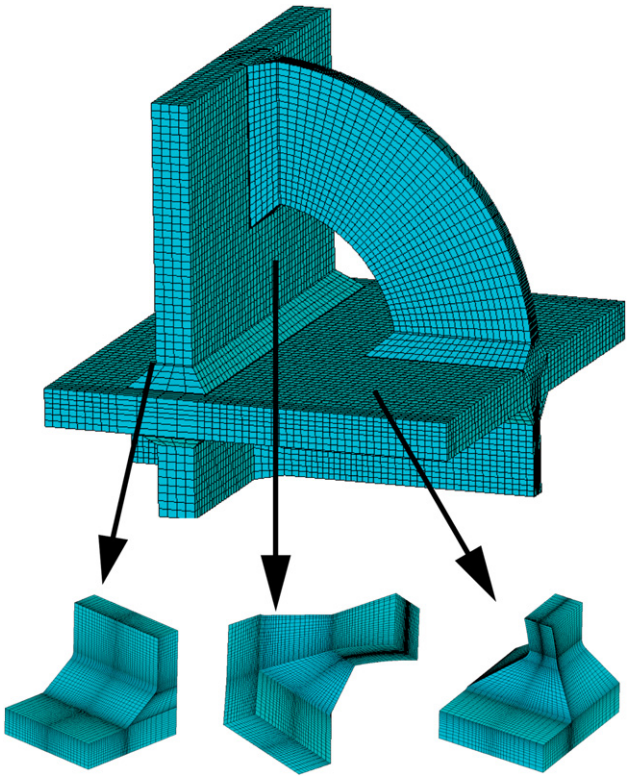

Fig. 9. Submodels for the calculation of notch stresses.

The effective notch stress was computed at the four hot-spots using the submodel technique in two steps by creating at first a refined model around the cut-out and afterwards four local models of the weld toes, see Fig. 9. The submodels were subjected at their boundary to displacements from the superior models. The element sizes were chosen according to [13]. Notch stresses were analysed in

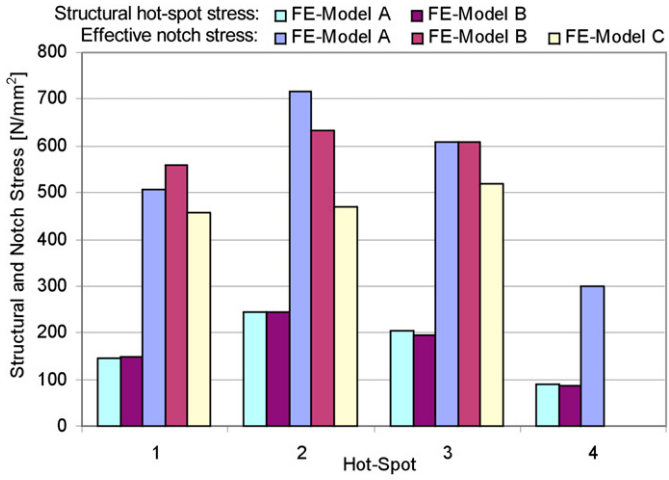

Fig. 10. Computed structural hot-spot and effective notch stresses for three weld geometries at HS1–HS4 for $\Delta F = 200$ kN.

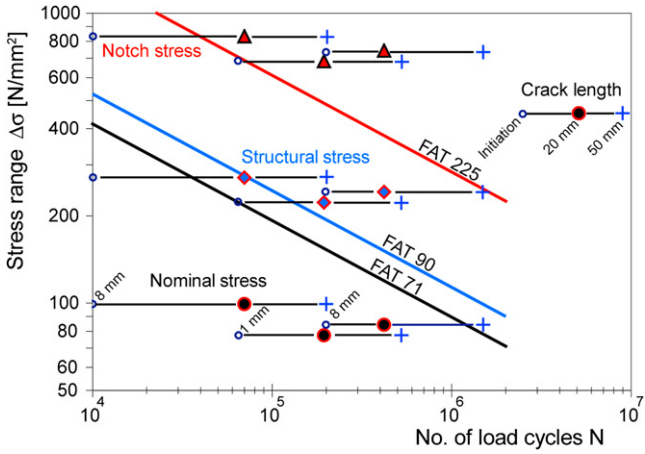

Fig. 11. S–N diagram for the critical web frame corners on the basis of nominal, structural hot-spot and effective notch stresses (20 mm crack length especially marked).

models A and B using the reference radius $r_{ref} = 1$ mm [11], which corresponds to the worst case in the approach proposed by Radaj [5], assuming an actual weld toe radius $r = 0$ mm increased by 1 mm to account for micro-structural support effects of the material. In model C, the minimum value of the measured weld toe radii in the fatigue-critical region was applied, increased by 1 mm according to [5] as well.

Fig. 10 shows the computed structural hot-spot and effective notch stresses in the weld toes (max. principal stresses). Almost all analyses show that the highest stress occurs at HS2, as mentioned before. The differences between the two models A and B, i.e. the effect of the actual leg length, are small. However, pronounced differences can be seen in model C, where the actual weld toe radius is included and the highest notch stress now occurs at HS3. Particularly the large radius measured at HS2 (2.2 mm) reduces the notch stress here so that also this can be the reason for the high fatigue strength of this location. The favourable shape of the weld toe (see Fig. 8) is influenced by gravity effects during welding, an effect which has been observed already in earlier investigations of bracket toes [14].

2.5. Discussion of the results

Using the computed nominal stress at the flange intersection and the structural hot-spot and notch stresses at HS3 in model B, the fatigue lives from the tests are plotted in the S–N diagram in Fig. 11 and compared with the design S–N curves of the different approaches [11], i.e. with FAT 71 for the nominal stress approach (cruciform joint), FAT 90 for the structural hot-spot stress approach (partial load-carrying fillet weld) and FAT 225 for the effective notch stress approach.

The results for the structural hot-spot and effective notch stress approach are on the safe side for the failure criterion chosen (crack length = flange thickness). Hence, the tests confirm the approaches. However, the results for the nominal stress approach are non-conservative. The main reason for this is the considerably reduced effective width which increases the stress in the middle of the flanges.

3. Intersection between longitudinals and transverse webs

3.1. Test models

A large number of failures occurred in large tankers built in the 1970s and 1980s particularly at the ship's sides at the intersection of longitudinals with transverse structures [15]. Fatigue cracks

normally appear at the end of the buckling stiffener attached to the top of the angle bar (hot-spots HS1 and HS2 in Fig. 12) and grow towards the side shell causing leakage. An underestimation of wave pressure loads and of secondary bending effects due to the asymmetric angle bars were identified as the main reasons. But also additional stresses due to the increased flexibility played a role.

However, this type of failure occurred more recently also in relatively large containerships using angle bars for the longitudinals. Here, additional warping stresses due to torsional loading were claimed to contribute to the failures [10]. The question was raised if these failures are certainly excluded in mid-sized containerships built in Germany, where so-called Holland profiles (bulb flats) are used for the longitudinals instead of angle bars, having only a slightly asymmetric shape. Therefore, it was decided to perform additional experimental and numerical investigations for this detail within the cluster project mentioned in the beginning.

In order to simulate the loading, a test rig with 3-point-bending of the longitudinal was set-up, see Fig. 13. A Holland profile HP 200 × 9 was chosen for the longitudinal, which was simply supported with hinges at the ends. At the top of the buckling stiffener (flat bar 150 × 10), which is placed on the transverse web (10 mm), a vertical force was acting via a hydraulic cylinder, creating a bending moment and a shear force in the longitudinal. The web was horizontally guided to avoid unrealistic, global rotation.

The location of the transverse web and the cylinder force were chosen such that a similar stress distribution occurs in the longitudinal as in the situation with a continuous longitudinal subjected to lateral pressure forces.

In total five test models were fabricated, three for constant and two for variable amplitude tests. Higher-tensile ship structural steel of grade A36 has been chosen, having a nominal yield strength $R_{eH} = 355$ N/mm^2. A reinforced throat thickness of $a = 4.5$ mm was realised for the welded connection between the buckling stiffener and the longitudinal in order to avoid cracks initiating from the non-welded root face. In addition to the direct connection between longitudinal and transverse web, a so-called lug was arranged as shown in Fig. 13.

3.2. Static pre-tests

During static pre-tests, all strains were checked to ensure realistic conditions. An interesting effect was extensive yielding during the first loading observed at the strain gauges applied directly in front of the weld toes HS1 and HS2. Fig. 14 shows the strain in these gauges for a loading up to 40 kN, which

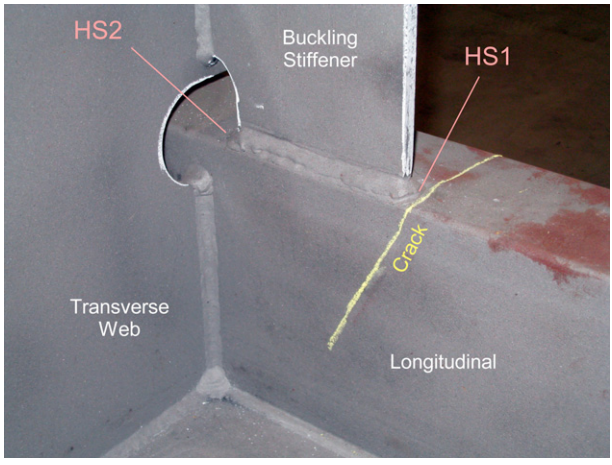

Fig. 12. Typical fatigue failure at a longitudinal (angle bar).

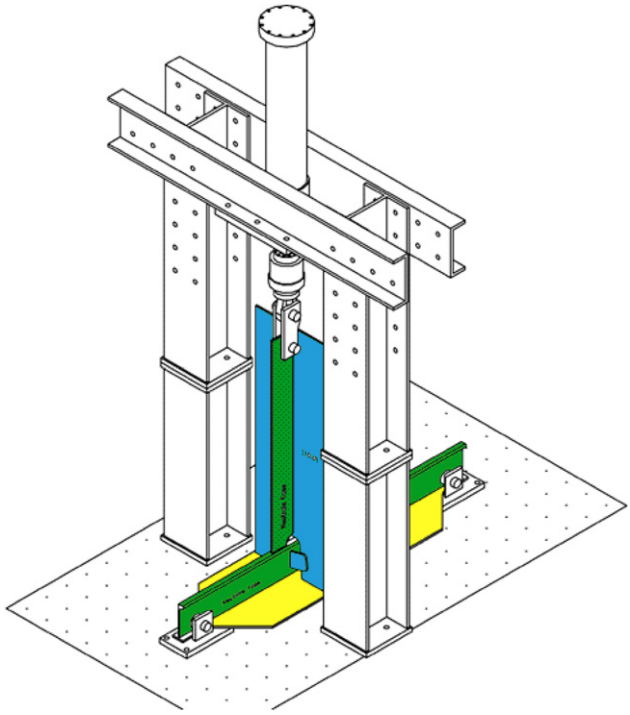

Fig. 13. Rig for the tests of the longitudinal/transverse web intersection.

corresponds to a nominal bending stress of only 75 N/mm^2. High local yielding occurs particularly at HS2. It should be noted that the non-linear behaviour has been observed only during first loading. The obvious reason for this are high tensile residual stresses caused by welding, which make the load-induced stresses reach the yield point at a fairly low level.

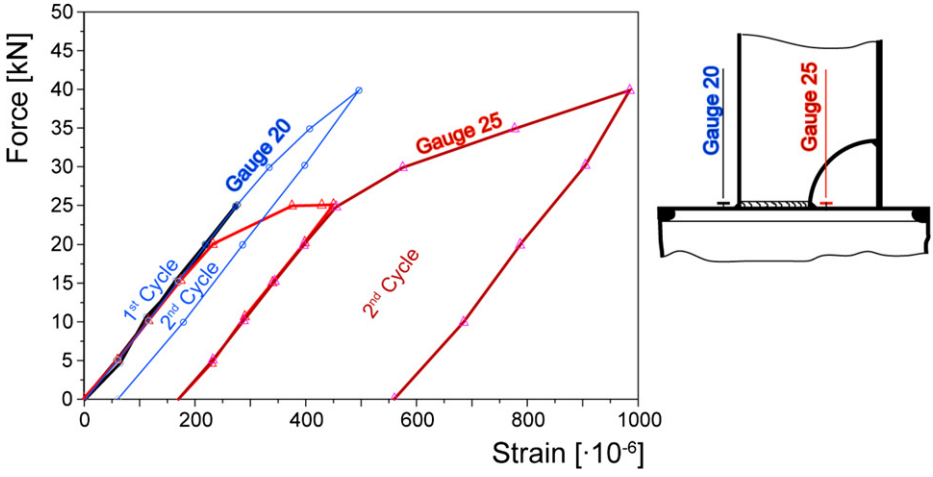

Fig. 14. Measured local strain at hot-spots HS1 (gauge 20) and HS2 (gauge 25) during first loading and unloading.

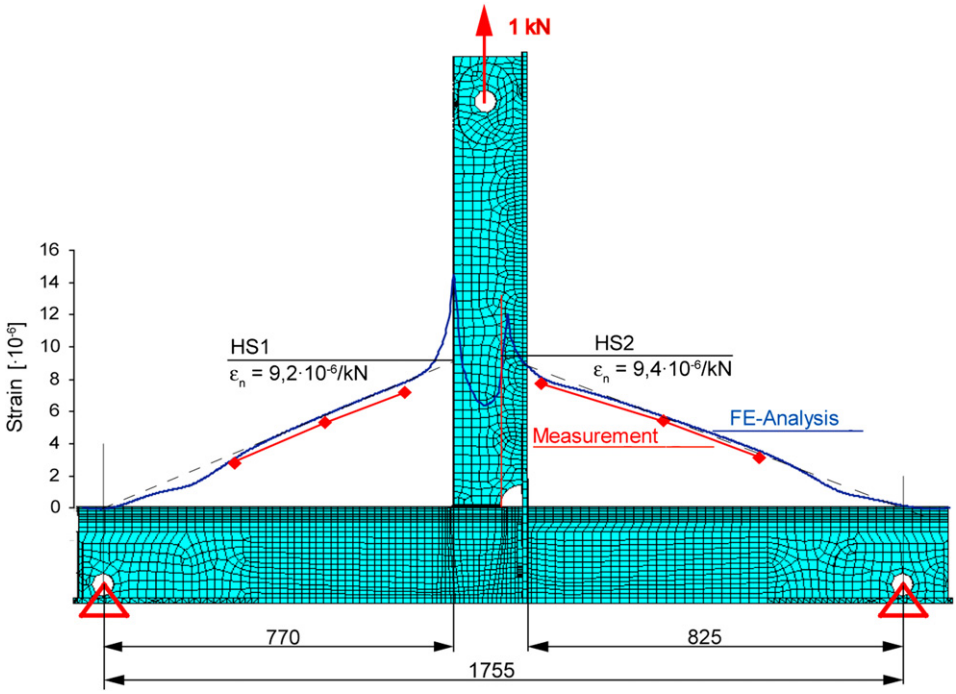

Fig. 15. Computed and measured global strain distribution in the test model.

3.3. Finite element analyses

Finite element analyses were performed in order to check the stress distribution and deformations in the model and to compute local stresses at the critical hot-spots, i.e. structural hot-spot stresses and effective notch stresses in accordance with current guidelines [4,13]. Fig. 15 shows the distribution of

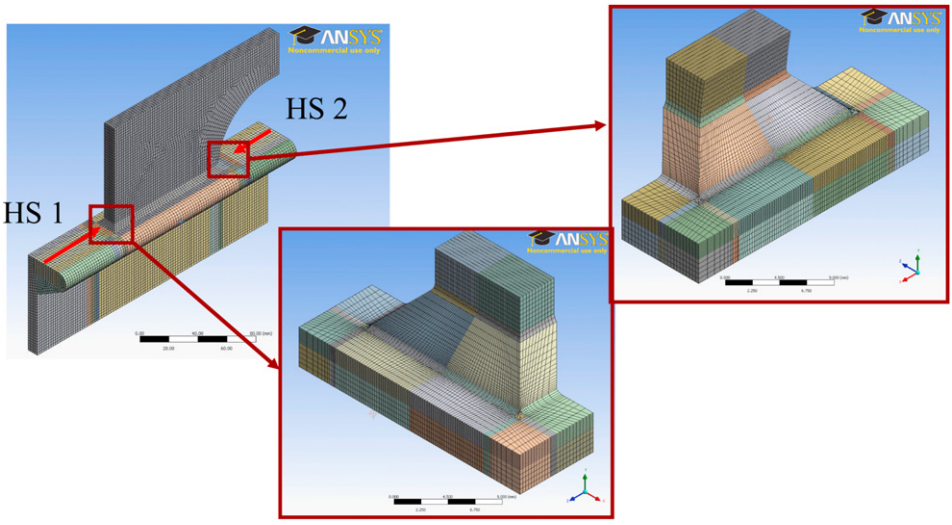

Fig. 16. Submodels for the computation of effective notch stresses.

Table 2
Computed nominal, structural hot-spot and effective notch stress for $F = 1$ kN.

Location	Nominal stress σ_n [N/mm^2]	Structural hot-spot stress σ_{hs} [N/mm^2]	Effective notch stress σ_k [N/mm^2]
HS1	1.93	4.21	9.91
HS2	1.92	3.82	8.81

the computed strains at the top of the Holland profile together with some measurement results. It can be seen that the linear strain distribution is somewhat disturbed in way of the hinges and also close to the intersection with the transverse web.

The computation of structural hot-spot stresses, which disregard the local stress peak at the weld toe by extrapolation of surface stresses to this point, creates some problems for weld toes on the surface of a bulb with respect to the definition of stress extrapolation points. However, the weld notches at the buckling stiffener toes can be regarded as in-plane notches because they are in the same plane as the web of the Holland profile. Therefore, a quadratic extrapolation over three points, located 4 mm, 8 mm and 12 mm away from the weld toe according to [4,11] has been chosen (along arrows in the left part of Fig. 16). This extrapolation scheme has been shown in [14] to give conservative results for attachments on bulbs of Holland profiles.

The effective notch stress was again computed with submodels having a mesh density which allows the weld toe to be fictitiously rounded with a reference radius of $r_{ref} = 1$ mm [13]. As shown in Fig. 16, two levels of submodels were necessary, being loaded by prescribed displacements taken from the superior models. Table 2 shows the computed nominal, structural hot-spot and effective notch stresses at the two critical locations. Remarkable is the relatively high increase of the structural stress compared to the nominal stress.

3.4. Constant amplitude fatigue tests

Models 1–3 were tested with constant amplitude loading. The applied force range for these models was 78 kN, 74 kN and 69 kN. The load ratio was approximately $R \approx 0$.

In Model 1, the first crack appeared almost simultaneously at HS1 and HS2, while the other models showed the first crack either at HS1 or HS2. The crack propagation phase was again rather long, as shown in Fig. 17 by the development of cracks in model 1. A substantial weakening of the model did not occur before the bulb of the profile was almost separated.

Although this was the end of the test, a reasonable failure criterion was considered to be a crack length on the bulb surface of 20 mm, corresponding to the overall weld width on the profile bulb. The number of cycles to this failure is summarized in Table 3. The results for the most critical location are also shown in

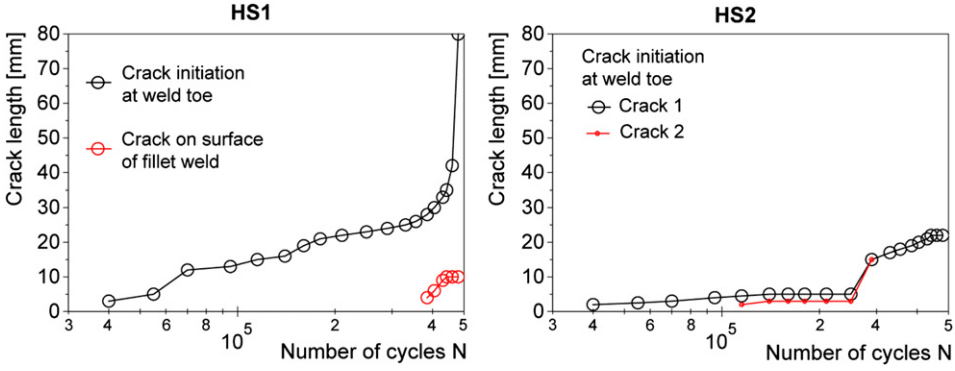

Fig. 17. Crack development in model 1.

Table 3
No. of cycles to failure (crack length 20 mm) in the fatigue tests.

Model no.	Constant/ variable amplitudes	(Max) force range ΔF [kN]	No. of cycles N at HS1 (incl. omitted ones)	No. of cycles N at HS2 (incl. omitted ones)
1	CA	78	180,000	405,000
2	CA	74	200,000	240,000
3	CA	69	Not reached	360,000
4	VA	150	28,520,000	Not reached
5	VA	122	300,400,000	300,400,000

the left part of the S–N diagram in Fig. 18 using the computed nominal, structural hot-spot and effective notch stresses. These are on the conservative side in comparison with the design S–N curves, i.e. FAT 56 for the nominal stress approach and this detail [6], FAT 100 for the structural hot-spot stress approach assuming a 100 mm long edge attachment [11] and again FAT 225 for the notch stress approach.

3.5. Variable amplitude fatigue tests

Two additional variable amplitude tests were performed to verify that the results from constant amplitude tests can be used for a fatigue assessment using the Palmgren–Miner rule to account for variable amplitudes.

Cyclic stresses are induced in longitudinals mainly by the seaway in the form of pressure fluctuations and global hull girder loads. Measurements, which have been summarized in [16], have shown that wave-induced loads are mostly distributed such that the spectrum is close to a straight line over the long term. This spectrum can be interpreted by the summation of several Gaussian distributions representing the effects of individual storms.

The corresponding WASH standardized load sequence has been chosen for the tests [17]. One load sequence includes 500,000 load cycles. In order to save testing time, all load cycles below 11% of the

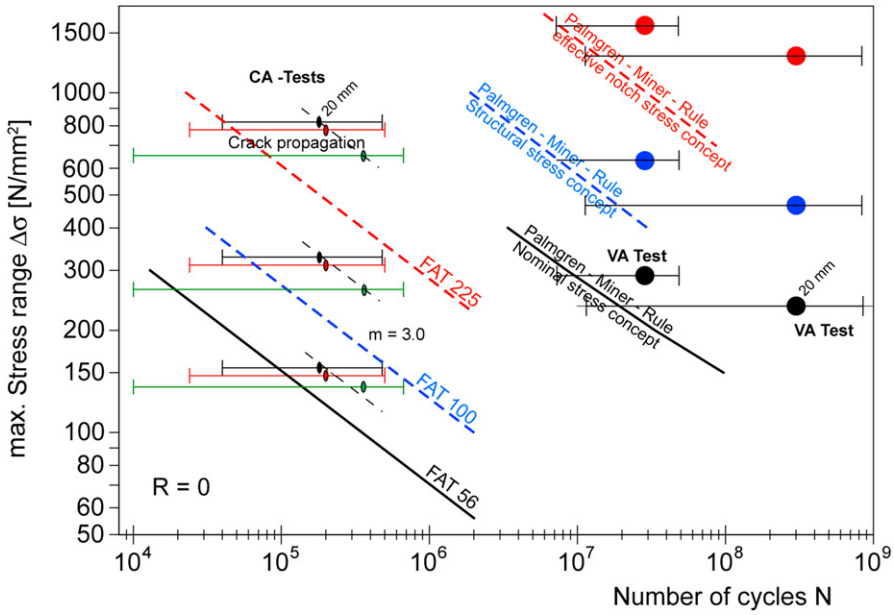

Fig. 18. Fatigue test results (for constant and variable amplitude tests; 20 mm crack length marked), design S–N curves based on different stress types and life curves using Palmgren-Miner rule.

highest load were omitted. However, all load cycle numbers given hereon refer to the original numbers.

In model 4, the first crack appeared after 7,290,000 load cycles at HS1, while model 5 showed the first crack after 10,150,000 load cycles at HS2. Again, a long crack propagation phase was observed until a crack length of 20 mm was reached according to the failure criterion chosen and also until the bulb was almost separated. The lives are given in Table 3 and shown in the right part of Fig. 18.

The fatigue life for the spectrum chosen was determined also with the Palmgren-Miner rule, using the mean S–N curves of the constant amplitude tests with a slope exponent $m = 3$, Haibach's correction and a damage sum $D = 0.5$ to account for uncertainties of the Palmgren–Miner Rule [11]. The results in Fig. 18 show a good agreement with the variable amplitude tests. This means that the fatigue life can be well assessed using the common procedures based on the linear damage accumulation rule according to Palmgren and Miner.

4. Summary and conclusions

Ship structural details are prone to fatigue due to fluctuating loads, normally caused by the seaway, and due to relatively severe notches at the welded joints. Two typical details were investigated with full-scale tests and numerical analyses in a joint research programme to validate the current approaches for fatigue strength assessment. The following conclusions are drawn from the investigations:

- The initiation of the first cracks in the tests was followed by a long crack propagation phase until the structure was substantially weakened. A reasonable failure criterion, corresponding to fractures in small-scale specimens, was considered to be a crack length of 20 mm, i.e. the thickness of the flange or alternatively the width of the weld at the attachment end considered.
- The numerical analysis of the structural hot-spot stress requires special considerations in some cases, such as for attachments on the bulb of Holland profiles. The stress extrapolation points have been chosen for in-plane attachments.
- The computation of the effective notch stress in large structures is possible with the help of the submodel technique, requiring more effort than the other techniques. However, it allows the effects of a local weld profile and increased weld toe radii to be considered.
- The fatigue assessment with the different approaches, including the Palmgren–Miner Rule for variable amplitude loading, gives results on the conservative side. An exception is the nominal stress approach in case of web frame corners, where a reduced effective width results in a non-conservative assessment if this is not considered.
- The failure behaviour of complex structures determined in numerical analyses may differ from the actual failure behaviour due to varying residual stresses which may cause hot-spots to be less critical than assumed for the presence of very high residual stresses.
- The question regarding the vulnerability of longitudinals made of Holland profiles can be answered by all approaches which are able to consider the occurring high structural stress concentration appropriately.

Acknowledgement

The investigations were performed within the project "Stiffened plate structures in shipbuilding" which was funded with public means within the programme "Industrial Cooperative Research" by the German Federal Ministry of Economics and Technology via the AiF and was coordinated by the Center of Maritime Technologies (CMT) in Hamburg. The fabrication of the test models by Flensburger Schiffbau-Gesellschaft and TKMS Nordseewerke in Emden is highly appreciated.

References

[1] Fricke W, Petershagen H, Paetzold H. Fatigue strength of ship structures – part 1: basic principles. Hamburg: GL-Technology, Germanischer Lloyd; 1997.

[2] Fricke W. Recommended hot-spot analysis procedure for structural details of ships and FPSOs based on Robin FE analyses. Int. J. Offshore Polar Eng. 2002;12:40–7.
[3] Fricke W. Fatigue of welded joints: state of development. Marine Structures 2003;16:185–200.
[4] Niemi E, Fricke W, Maddox SJ. Fatigue analysis of welded components – designer's guide to the hot-spot stress approach. Cambridge: Woodhead Publ.; 2006.
[5] Radaj D, Sonsino CM, Fricke W. In: Fatigue assessment of welded joints by local approaches. 2nd ed. Cambridge: Woodhead Publishing; 2006.
[6] Germanischer Lloyd. Rules and guidelines, I - ship technology, part 1 – seagoing ships, chapter 1 - hull structures. Hamburg: Germanischer Lloyd; 2008.
[7] Germanischer Lloyd. Rules and guidelines, V - analysis techniques, chapter 2 - guidelines for fatigue strength analyses of ship structures. Hamburg: Germanischer Lloyd; 2004.
[8] Det Norske Veritas. Fatigue design of offshore steel structures, Recommended practice DNV-RP-C203. Høvik: Det Norske Veritas; 2008.
[9] Common structural rules. International Association of Classification Societies (IACS), http://www.iacs.org.uk/publications/default.aspx; 2007.
[10] Müller L. Erklärung für Risse in großen Containerschiffen (Explanation for cracks in large containerships). Schiff & Hafen 2003;12:30–1.
[11] Hobbacher, H., Recommendations for fatigue design of welded joints and components. IIW doc.1823-07, Welding Research Council Bulletin 520, New York; 2009.
[12] Fricke W, von Lilienfeld-Toal A, Paetzold H. Versteifte Plattenstrukturen im Stahlschiffbau - im Cluster Anwendbarkeit von Festigkeitskonzepten für schwingbelastete, geschweißte Bauteile, CMT-Report 14/2009. Hamburg: Center of Maritime Technologies; 2009.
[13] Fricke W. Guideline for the fatigue assessment by notch stress analysis for welded structures. International Institute of Welding; 2008. IIW-Doc. XIII-2240r1-08/XV-1289r1-08.
[14] Fricke W, Kahl A. Local stress analysis and fatigue assessment of bracket toes based on measured weld profile. International Institute of Welding; 2007. IIW-doc. XIII-2166-07/XV-1253-07.
[15] Yoneya T, Kumano A, Yamamoto N, Shigemi T. Hull cracking of very large ship structures. In: Proceedings of fifth international conference on integrity of offshore structures, Glasgow. London: Engineering Materials Advisory Services; 1993.
[16] Fricke W, von Lilienfeld-Toal A. Annahmen von Beanspruchungskollektiven für Schiffskonstruktionen und deren Absicherung durch Messung (Assumptions of stress spectra for ship structures and their validation by measurement). MP/Materials Testing 2008;50:721–8.
[17] Schütz W, Pook LP, Dover WD. Progress in the development of a Wave Action Standard History (WASH) for fatigue testing of tubular structures in the North Sea. In: ASTM symposium on development of fatigue loading spectra, Cincinnatti; 1987.